300 m. Recall that it was at this depth, at the Cluster C site (15°N), that a critical layer was observed. Remarkably, $Q_y \rightarrow 0$ at the Cluster C latitude. Indeed, close examination of the $Q_y(z)$ profile (Figure 2) used in Keffer (1982a) to calculate shear modes, shows that the sign reversal happens at 300 m. This comes from a completely independent data set using NODC Nansen bottle data.

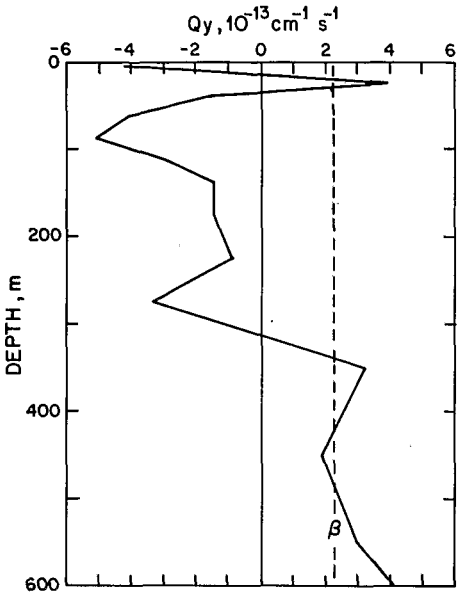

FIGURE 2 *(Keffer)*
Northward potential vorticity gradient (Q_y) calculated as $Q_y = \beta - (f\bar{\rho}_y/\bar{\rho}_z)_z$ from historical data (Keffer, 1982b). The dashed line is the planetary vorticity gradient β. Note that $Q_y \rightarrow 0$ at 300 m.

Pedlosky (1982) described a two-layer model in which a critical layer and a weak potential vorticity gradient are present in the lower layer. The mean shear is slightly supercritical. In the limit of low frequency, slightly dissipative waves, an instability develops, grows, and then feeds back to the mean flow and potential vorticity gradients, resulting in a finite-amplitude state where the potential vorticity gradient in the lower layer (*i.e.*, the critical layer) has been homogenized. Although this is a simple model, more physical arguments, such as Bretherton's (1966), would also suggest that potential vorticity gradients within a critical layer may be especially susceptible to erosion and eventual homogenization due to the large particle excursions in the layer.

Cluster C is located far downstream in a 2500 km long current, and most likely will be observing the finite-amplitude state of any developing waves and resulting potential vorticity gradient. Indeed, no significant downgradient heat fluxes were observed (Keffer, 1982b).

Two additional questions suggest themselves. First, from Figure 1, it can be seen that the isopycnal $\sigma_\theta = 26.8$ that is suspected of containing a critical layer at the Cluster C laititude and where $Q_y \rightarrow 0$, is the same isopycnal that has undergone extensive homogenization within the subtropical gyre (latitudes 20°-36°) due to processes described by Rhines and Young (1982). This may be coincidence or it may be due to the interactions between the two processes.

Second, although the condition $Q_y \rightarrow 0$ at z_c removes the requirement for critical layer instability, it is unclear what it implies for baroclinic instability in general.

References

Bretherton, F. P. (1966) Critical layer instability in baroclinic flows. *Quarterly Journal of the Royal Meteorological Society, 92,* 325-334.

Keffer, T. (1982a) Time dependent temperature and vorticity balances in the Atlantic North Equatorial Current. *Journal of Physical Oceanography,* in press.

Keffer, T. (1982b) The baroclinic stability of the Atlantic North Equatorial Current. *Journal of Physical Oceanography,* submitted.

McDowell, S. E., P. B. Rhines and T. Keffer (1982) Maps of potential vorticity in the North Atlantic and their relation to the general circulation. *Journal of Physical Oceanography,* in press.

Pedlosky, J. (1982) A simple model for nonlinear critical layers in an unstable baroclinic wave. *Journal of Fluid Mechanics,* in press.

Rhines, P. B. and W. R. Young (1982) Homogenization of potential vorticity in planetary gyres. *Journal of Fluid Mechanics,* in press.

Tom Keffer
Department of Physical Oceanography
Woods Hole Oceanographic Institution
Woods Hole, MA 02543

The 1978 Occurrence of High Sea Surface Salinity in the Eastern Coral Sea

Long-term changes in sea surface salinity in the Coral Sea, including high salinity values occurring in the periods 1957-58 and 1972-73, have been described by Donguy and Henin (1975). These phenomena were related to the El Niño events along the western coast of South America (Donguy and Henin, 1981). During these periods the Intertropical Convergence Zone (ITCZ) was on the equator and the eastward flowing South Equatorial Countercurrent (SECC) was particularly noticeable north of 10°S. South of this latitude a strong westward current advected high salinity waters. At the same time, drastic drought conditions occurred in southwest Pacific countries.

During 1978, when high sea surface salinities were observed (Figure1) in the eastern Coral Sea, the El Niño phenomenon did not occur in the eastern Pacific Ocean. In this note an attempt is made to determine whether changes in the current system explain the salinity variation. Generally, in the southwest Pacific Ocean, eastward flows carry low salinity water and westward flows transport saltier water.

The mean height of the surface dynamic topography relative to 1000 decibars is quite variable in the Coral Sea. A zonal ridge is commonly observed near 15-18°S, inducing an eastward flow on the south side (the South

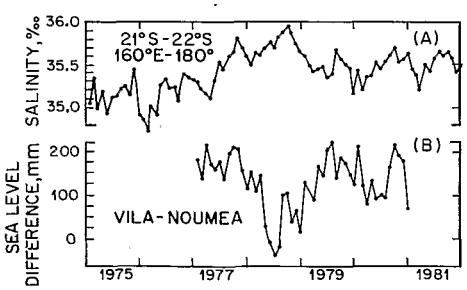

FIGURE 1 *(Henin)*
(A) Monthly mean sea surface salinities recorded 1975-81 by merchant ships between 21°S-22°S and 160°E-180°. (B) Monthly mean sea level differences between Vila (17°26.4'S, 168°11.4'E) and Noumea (22°10.8'S, 166°15.6'E) during 1977 to 1981.

Tropical Countercurrent, STCC), a westward flow on the north side (the South Equatorial Current, SEC) and the eastward flowing South Equatorial Countercurrent (SECC) which passes through the Solomon Archipelago.

Scarcity of hydrological casts in the Coral Sea prompted the development of data collection using XBT measurements from merchant ships. In this way, data have been collected routinely along shipping lanes between New Caledonia and Japan, New Guinea, Vanuatu and Fiji (Meyers and Donguy, 1980). However, the XBT program only became operational in 1979, so no data are available to infer the current system during 1978 when the high salinities were observed.

The relationship between monthly mean values of dynamic height and sea level in tropical areas (Wyrtki, 1980) was exploited to monitor the current system variations in the Coral Sea. Sea level data from three stations were used. Honiara (Solomon Islands) lies in the dynamic trough between the SECC and the

curves σ_o and σ_p. This suggests that about half of the remaining variability for this model is accounted for by changes in SST between the equator and 30°N.

These conclusions are further supported by a more comprehensive study by Manabe and Hahn (1981) who integrated the GFDL (Geophysical Fluid Dynamics Laboratory) spectral climate model for 15 years with prescribed but seasonally varying boundary condition of SST. They found that the ratio of zonally averaged values of standard deviation of seasonal mean for observations and model simulations was about two in the near equatorial regions and reduced to about one in the middle and high latitudes.

This supports our earlier hypothesis that the slowly varying boundary conditions play an important role in determining the interannual variability of time averages for the tropics. Additional effects of soil moisture (Shukla and Mintz, 1982) or snow cover could possibly bring the σ_o and σ_B curves still closer. It is however to be noted that the long period internal dynamical changes (tropical-extratropical interactions, *etc.*) also contribute to the interannual variability of time averages, and boundary forcings alone cannot explain the total observed variance.

It is reasonable to conclude that although for short and medium range the instantaneous state of the tropical atmosphere is less predictable, the time averages (monthly and seasonal means) are potentially more predictable in the tropics. Since there is sufficient observational, theoretical and numerical model experimental evidence that tropical heat sources can also influence the middle latitude circulation, it is likely that the monthly means for middle latitudes could also be potentially predictable due to their interaction with low latitudes.

References

Charney, J. G., R. G. Fleagle, V. E. Lally, H. Riehl and D. Q. Wark (1966) The feasibility of a global observation and analysis experiment. *Bulletin of the American Meteorological Society, 47,* 200-220.

Charney, J. G. and J. Shukla (1981) Predictability of monsoon. In: *Monsoon Dynamics,* J. Lighthill and R. P. Pearce, editors, Cambridge University Press, Cambridge, 99-109.

Lorenz, E. N. (1969) The predictability of a flow which possesses many scales of motion. *Tellus, 21,* 289-306.

Manabe, S. and D. G. Hahn (1981) Simulation of atmospheric variability. *Monthly Weather Review, 109,* 2260-2286.

Shukla, J. (1981) Predictability of the tropical atmosphere. NASA Technical Memorandum 83829, Laboratory for Atmospheric Sciences, NASA Goddard Space Flight Center, Greenbelt, MD, 51 pp.

Shukla, J. and Y. Mintz (1981) The influence of land-surface evapotranspiration on the earth's climate. *Science, 215,* 1498-1501.

Smagorinsky, J. (1969) Problems and promises of deterministic extended range forecasting. *Bulletin of the American Meteorological Society, 50,* 286-311.

Jagadish Shukla
Laboratory for Atmospheric Sciences
NASA/Goddard Space Flight Center
Greenbelt, MD 20771

Erosion of Potential Vorticity Gradients by Critical Layers in the Atlantic North Equatorial Current

Bretherton (1966) showed that the presence of a critical layer, which occurs at depth z_c when $\bar{U}(z_c) = c_p$, where $\bar{U}(z)$ is the zonal mean flow profile and c_p is a disturbance phase speed, implies the instability of the flow. At depth z_c the particle speed equals the phase speed and a given particle is always exposed to the same phase of a wave cycle. Particles which are initially moving north will continue to do so, and conversely, southward moving particles continue to move south. These excursions imply a large north-south flux of potential vorticity *unless* the potential vorticity gradient (Q_y) vanishes at z_c. If $Q_y \neq 0$, the resulting flux of potential vorticity can only be balanced by growth of the instability.

Using the POLYMODE Array III Cluster C data set, Keffer (1982a) found four independent pieces of evidence for the existence of a critical layer at 300 m depth within the Atlantic North Equatorial Current. (1) The 3.5 cm s^{-1} westward cross-correlation phase velocity corresponds to the 300 m flow velocity. (2) The primary temperature balance at 300 m is $T'_t + \bar{U}T'_x = 0$, where T' is the temperature perturbation measured at the current meters. (3) The moored temperature measurements indicated a maximum eddy potential energy at 300 m. (4) Historical Nansen bottle data from the National Oceanographic Data Center (NODC) indicated a maximum eddy potential energy at 300 m.

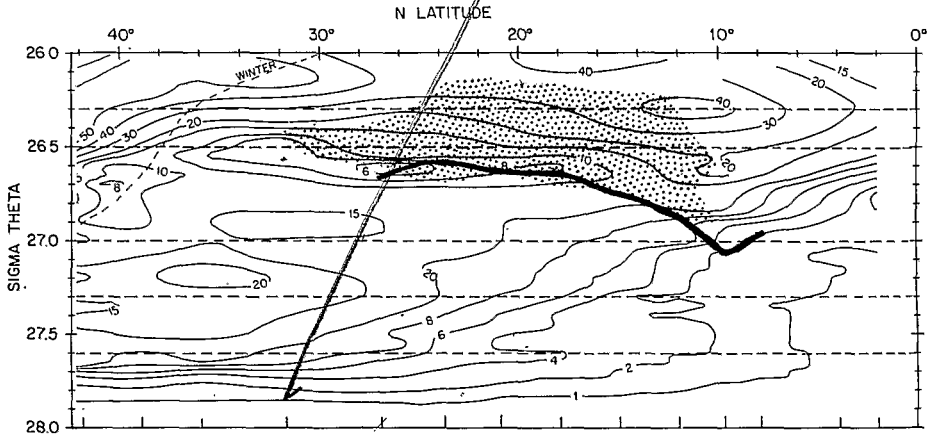

FIGURE 1 *(Keffer)*

Potential vorticity (10^{-13} cm^{-1} s^{-1}) along 50°W computed from GEOSECS data and contoured as a function of density (σ_θ) and latitude. The stippled region is where $Q_y < 0$ and these latitudes will be a likely site of baroclinic instability. Just below this region is a heavy solid line that marks the 300 m isodepth. Note that at 15°N, $Q_y \rightarrow 0$ at this depth. This may be due to critical layer homogenization. The dashed line is the winter outcrop.

Given the existence of a critical layer and the importance of the north-south eddy flux of potential vorticity, it becomes important to ask: What is the mean potential vorticity gradient at z_c?

Figure 1 is a contour plot of potential vorticity along the GEOSECS cruise track (~50°W) in the western Atlantic from McDowell *et al.* (1982). Potential vorticity was evaluated from

$$Q = -\frac{f}{\rho}\frac{\partial \rho_\theta}{\partial z}$$

where $\partial\rho_\theta/\partial z$ is the vertical adiabatic density gradient, ρ is the density and f is the Coriolis parameter. In Figure 1, Q is contoured as a function of surface referenced density anomaly (σ_θ) and latitude. Such a prescription for Q is consistent for large scale slow motions where relative vorticity and horizontal components of vorticity are small.

Also shown in the North Equatorial Current area is a curve representing the density at

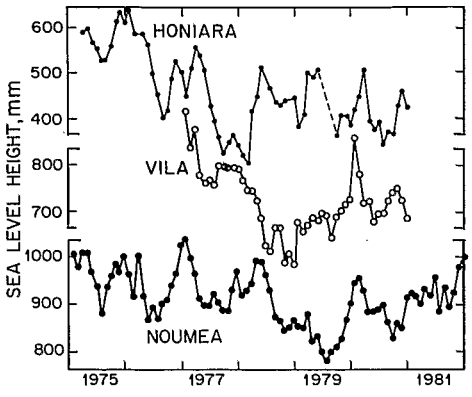

FIGURE 2 *(Henin)*
Monthly mean sea level values recorded at Honiara (9°15.6'S, 159°34.2'E), Vila (17°26.4'S, 168°11.4'E) and Noumea (22°10.8'S, 166°15.6'E).

SEC. Vila (Vanuatu) is located either on the ridge between SEC and STCC or on the north side of the eastward STCC. Noumea (New Caledonia) has always been observed to be in the STCC.

Because of the uncertain location of the ridge between 15°S and 18°S, the sea level difference is significant only between Vila and Noumea, which are always in the south eastward flux. Available time series of mean sea levels for the 1975-81 period are shown in Figure 2. Using harmonic analysis, Wyrtki (1980) showed annual and semi-annual sea level variations at Honiara and Noumea. These variations are masked by a southward travelling low sea level disturbance which was recorded in late 1977 at Honiara, in late 1978 at Vila and in mid 1979 at Noumea. In order to eliminate the variations of periods shorter than one year, a twelve month running mean was used before computing cross-correlation coefficients between Honiara and Vila, Vila and Noumea, and Honiara and Noumea. The largest correlation coefficients were obtained at lags of 11 months for Honiara-Vila, 5 for Vila-Noumea and 16 for Honiara-Noumea, indicating a southward movement of the low sea level disturbance of about 4 cm s^{-1}.

The geostrophic flow between stations is related to the difference of dynamic heights at these locations, so the relationship between dynamic height and monthly mean sea level allows us to use the difference of monthly mean sea level between two islands to monitor the magnitude of the geostrophic transport. Thus, the southward travelling low sea level disturbance observed in the Coral Sea produces a change in the current strength.

The sea level difference between Vila and Noumea (Figure 1), which is representative of the magnitude of the eastward flowing STCC, shows a very well marked minimum in 1978, which coincides with the sea surface salinity maximum near 21°S-22°S. Normally the eastward STCC carries low salinity water and moves at an average speed of 25 cm s^{-1}. However, in 1978 the rate of flow was considerably weaker, about 5 cm s^{-1}. It therefore seems that the higher salinities observed are a consequence of the smaller volume of low salinity waters being carried to the Coral Sea. The origin of the southward moving low sea level disturbance has not yet been elucidated.

References

Donguy, J. R. and C. Henin (1975) Surface waters in the north of the Coral Sea. *Australian Journal of Marine and Freshwater Research, 26,* 293-296.

Donguy, J. R. and C. Henin (1981) Two types of hydroclimatic conditions in the southwestern Pacific. *Oceanologica Acta, 4,* 57-62.

Meyers, G. and J. R. Donguy (1980) XBT monitoring by ship of opportunity. *Tropical Ocean-Atmosphere Newsletter,* No. 1.

Wyrtki, K. (1980) The Pacific NORPAX sea-level network. *Tropical Ocean-Atmosphere Newsletter,* No. 1.

Christian Henin
O.R.S.T.O.M.
B. P. A5
Noumea Cedex
New Caledonia

Drifting Buoy Clusters in the Atlantic Equatorial Undercurrent

The large horizontal shear of the jet-like Equatorial Undercurrent (EUC) could be the source of high horizontal mixing rates. Contrary to this concept is the occurrence of the narrow (*e.g.*, 200 km wide) high salinity core across the equatorial Atlantic (Katz *et al.*, 1980). Thus, two questions are raised: are high mixing rates compensated by the horizontal advection of meridional circulation cells and is horizontal mixing small enough to be neglected compared to the loss due to vertical mixing?

Four experiments with drifting buoy clusters were carried out in the equatorial Atlantic (Table 1) to measure horizontal turbulent diffusion rates. The 21 m^2 drogues (Figure 1) were located within the EUC. Ship's radar was used to track the surface buoys. Because of the relatively long (up to 6 hours) hiatus between the satellite fixes, one buoy is arbitrarily chosen from the cluster to be a reference buoy and the other buoys are positioned relative to the reference buoy every 30 minutes. The track of the reference buoy is determined relative to the ship, which itself is positioned by satellite navigation.

During the CIPREA experiment, simultaneous current measurements were carried out from the drifting ship to determine the vertical shear of the current. The current shear in the vertical direction induces an error in the absolute current measurement by the drogue because of the drag on the buoy and on the wire. The error calculated from the observed current shear is about 15%. The measurements

TABLE 1 *(Fahrbach)*
Drifting buoy experiments.

Experiment	*Number of buoys*	*Start time*	*Duration*	*Mean position*
CIPREA	6	1700 GMT 15 AUG 78	1.83 d	00°36'S 03°43'W
D1	9	1030 GMT 14 FEB 79	2.08 d	00°30'N 21°25'W
D2	8	1730 GMT 18 MAY 79	1.88 d	00°16'W 20°59'W
D3	5	1800 GMT 14 JUN 79	1.60 d	00°01'S 21°38'W

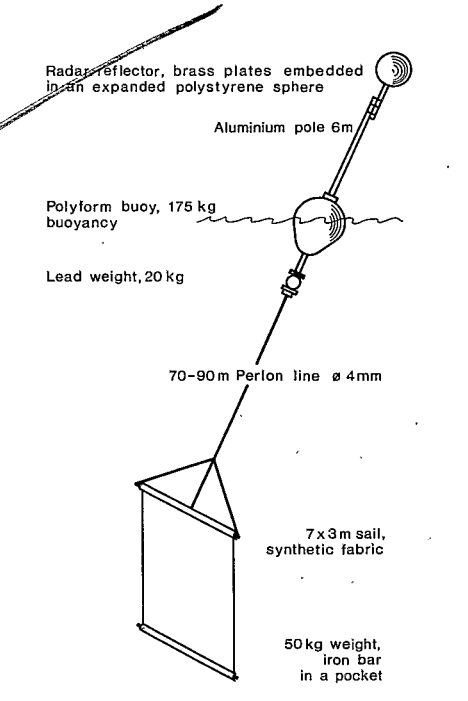

FIGURE 1 *(Fahrbach)*
Schematic representation of the buoys used to measure horizontal turbulent diffusion rates in the equatorial Atlantic.

Number 14, November 1982

FIRST CLASS MAIL

Dr. David Halpern
JISAO
University of Washington, AK–40
Seattle, WA 98195 U.S.A.

tropical
ocean-atmosphere
newsletter

The **Tropical Ocean-Atmosphere Newsletter (TO-AN)** is published bimonthly by the University of Washington's Joint Institute for the Study of the Atmosphere and Ocean (JISAO), with support from NOAA's Equatorial Pacific Ocean Climate Studies (EPOCS) Program, to provide timely dissemination of information about tropical atmospheric and oceanic research studies. Uncopyrighted articles and diagrams may be reprinted with appropriate citation. Material for publication, comments, and requests for subscriptions may be sent to Dr. David Halpern, JISAO, University of Washington, AK–40, Seattle, WA 98195, USA.

Meetings

AGU Fall Meeting, 7-15 December 1982, San Francisco

Sessions of interest are (a) the SEAREX program, (b) upper ocean dynamics and (c) equatorial dynamics. Contact American Geophysical Union, 2000 Florida Avenue N.W., Washington, DC 20009 (tel: 202-462-9603).

Second Conference on Climate Variations, 10-14 January 1983, New Orleans

Sessions of interest are (a) climate modeling and prediction, (b) climate variations, (c) the Southern Oscillation and (d) tropical sea surface temperature variations. Contact American Meteorological Society, 45 Beacon Street, Boston, MA 02108 (tel: 617-227-2425).

agree within this range.

The distribution of the buoy positions within a cluster is described in a Cartesian coordinate system with the origin at the center of gravity of the cluster. During the CIPREA experiment the spreading of the drifters seemed rather isotropic, whereas during D2 the spreading was dominated by strong horizontal north-south shear. These observations indicate the difficulty in separating influences due to space scales greater and smaller than the array size. Molinari and Kirwan (1975) and Okubo and Ebbesmeyer (1976) assumed a horizontally linear varying mean current to which a random turbulent velocity is added. Using the CIPREA and D2 measurements, the equations for the mean velocity components and their first horizontal derivatives are solved by minimizing the turbulent velocity term.

Experiment D1 was carried out between current meter moorings at the equator and at 1°N. The horizontal derivative calculated from the drifters and the moored current meters agrees witin the errors. This gives some confidence to the methods. The divergence of the mean field does not differ significantly from zero. This corresponds with the temperature observations that no significant cooling occurred during the experimental period. If we assume that the standard deviation of the drifter coordinates is equivalent to a mixing length and that the turbulent velocity is equal to the turbulence intensity, then the horizontal mixing coefficients can be calculated from the method described by Okubo and Ebbesmeyer (1976). The computed coefficients (Figure 2) agree with those given by Okubo (1971).

FIGURE 2 *(Fahrbach)*
Horizontal turbulent diffusion coefficients versus the horizontal scales of the clusters which are given by twice the mean distance of the buoys towards the center of gravity. The coefficients are marked with an x for the east-coordinate and with a y for the north-coordinate. The line represents a local fit to 4/3 power law given by Okubo (1971).

References

Katz, E. J., J. G. Bruce and B. D. Petrie (1980) Salt and mass flux in the Atlantic Equatorial Undercurrent. *Deep-Sea Research, GATE Supplement II, 26,* 137-160.

Molinari, R. and A. D. Kirwan, Jr. (1975) Calculations of differential kinematic properties from Lagrangian observations in the western Caribbean Sea. *Journal of Physical Oceanography, 5,* 483-491.

Okubo, A. (1971) Oceanic diffusion diagrams. *Deep-Sea Research, 18,* 789-802.

Okubo, A. and C. C. Ebbesmeyer (1976) Determination of vorticity, divergence and deformation rates from analysis of drogue observations. *Deep-Sea Research, 23,* 349-352.

Eberhard Fahrbach
Institut für Meereskunde
Universitat der Kiel
D 2300 Kiel 1
Federal Republic of Germany

tropical ocean-atmosphere newsletter

Number 14 November 1982

Energetic Propagating Sea Level Events Along the Pacific Coast of Mexico

Along low latitude ocean boundaries (including the equator), baroclinic long waves are a preferred mode of oceanic response to transient wind forcing. Poleward propagating disturbances with frequencies of 0.1-0.5 cpd and properties similar to those of internal Kelvin waves have been observed equatorward of 15°S along the Peru coast (Smith, 1978). The source of forcing for these waves—along the coast or in the equatorial waveguide—is not known and is one of the questions prompting current research. As such waves propagate poleward along an eastern boundary, the internal Rossby radius of deformation decreases with increasing latitude. When it is comparable to the offshore scale of the continental margin, the waves are theoretically expected to be more of a hybrid form, retaining some of the characteristics of internal Kelvin waves, while becoming more like topographically supported continental shelf waves. For typical topographic scales this transition should occur in the 10-20 degree latitude range (see, *e.g.*, Allen and Romea, 1980), though Brink (1982) finds that even at lower latitudes the waves are hybrids. Christensen and de la Paz (1982) have observed propagating sea level disturbances along the continental Pacific coast of Mexico between Salina Cruz (16°N) and Guaymas (28°N), and conclude that they have internal Kelvin wave characteristics (see locations in Figure 2). Their results are based primarily on a correlation analysis of year-long sea level records for 1971. From the lagged correlations they find poleward propagation speeds of 190-380 km day^{-1} (100 km day^{-1} = 1.16 m s^{-1}). They call attention to the existence of solitary, energetic events of elevation (10-30 cm) whose alongshore coherence and propagation are evident from time series plots. Their work leaves unanswered the questions of how and where these large amplitude disturbances are generated, and how their propagation characteristics agree or disagree with coastal trapped wave theory.

We have examined the 1971 data and find that the energetic events in that year were confined to the summer season (May-October), suggesting they are generated by eastern North Pacific tropical storms that normally occur in the same season. Figure 1 shows the sea level time series for the 1971 tropical storm season, spaced vertically in proportion to station separation. Single, coherent events aligned along straight off-vertical lines can be seen, indicating poleward propagation speeds of the order of 250 km day^{-1}. To document the atmospheric forcing of the events, we examined the eastern North Pacific storm tracks for the 1971 storm season. Compared with other years, 1971 was remarkable for the relatively large number of tropical storms and hurricanes that passed within 600 km of the Mexican coast. Nine tropical storms (most of them of hurricane intensity) coincided temporally and spatially with corresponding sea level events in the Acapulco-Manzanillo region; the tracks for these are shown in Figure 2. All storm centers passed within 500-600 km of the coast. The tracks are only plotted where tropical storm or hurricane force conditions were observed; hence, near-coastal intense storm activity was mainly limited to the region between Guatemala and Manzanillo.

To see if the forcing by tropical storms is further corroborated by coastal wind records, we examine the maximum daily wind speeds reported by Mexican airports at Salina Cruz, Acapulco, Mazatlan and Guaymas. We found that wind speeds significantly above the usual daily maximum had occurred at Acapulco and/or Salina Cruz, coinciding with the passage of storms and sea level events. The solid circles in Figure 1 show where both nearby tropical storms were reported, and coastal winds were stronger than usual. In contrast, during the periods of sea level event passage at Mazatlan and Guaymas, no significant local wind increases could be found. These results suggest that the energetic sea level events were gener-

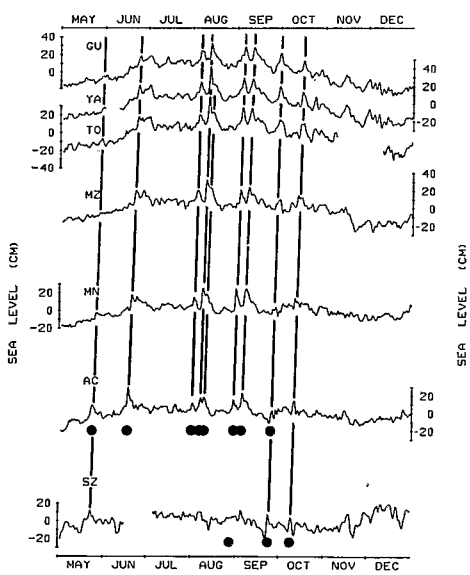

FIGURE 1 *(Enfield and Allen)*
Sea level records for 8 months in 1971 from stations along the Pacific continental coast of Mexico. Coherent propagating events of elevation are indicated by slanted lines. Solid circles indicate times and stations for which evidence of near coastal tropical storm activity was found.

CONTENTS

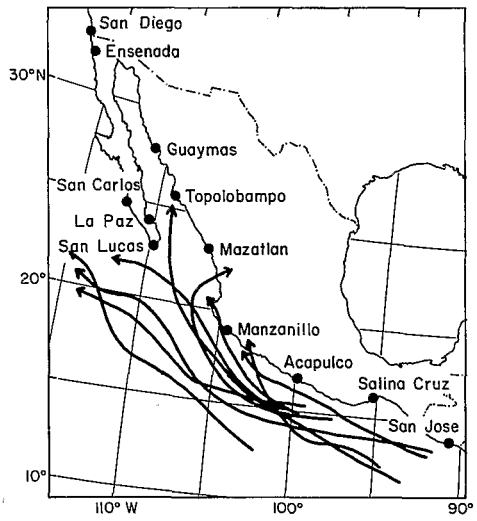

FIGURE 2 *(Enfield and Allen)*
Eastern North Pacific tropical storm tracks that passed within 600 km of the mainland coast of Mexico in 1971. Sea level stations are indicated by solid circles.

ated by storm activity along the southern Mexican coast, generally between Salina Cruz and Manzanillo, and subsequently propagated northwestward into the Gulf of California as freely propagating disturbances.

A number of additional questions are raised by the analysis of 1971 sea level: (1) Do similar energetic events occur during other years? Are they as frequent as in 1971, similarly confined to the May-October period, and generated by tropical storms? (2) Are the above (visual) indications of generation and propagation of coastal trapped waves confirmed by time series analysis? (3) How are the generation and propagation processes distributed across the frequency spectrum? (4) Are there significant seasonal differences in the occurrence of coastal trapped waves, in their propagation characteristics and/or their generation? (5) Are there any systematic variations in the propagation characteristics, from one part of the coast to another, that would suggest forced *versus* free wave propagation, and that would indicate the type of wave involved? In an attempt to answer these questions, we have studied sea level and wind records for a three-year period (1973-1975) from stations between San Jose, Guatemala (14°N) and Guaymas.

A detailed treatment of our work will appear in a later publication, but we can summarize some of our results here. Similar large amplitude, propagating sea level events do occur during other summers, less frequently than in 1971, but also associated with tropical storms and hurricanes. Cross-correlation and cross-spectral analyses confirm the existence of propagating waves and their generation by winds off southern Mexico. Coherence and phase spectra between sea level time series for five-month summer storm seasons show propagating wave activity over the entire frequency range resolved (0.03-0.14 cpd), but the coherences are strongest at lower frequencies (0.03-0.21 cpd). The sea level variability is less coherent alongshore during winter periods, giving fewer reliable estimates of propagation at all frequencies. Additionally, the winds at Acapulco are coherent with sea level during the summer seasons, but not during the winters. For the summer periods, the wave speeds found from cross-spectral analysis, and their latitudinal distribution, are similar to those found from an analysis of individual large amplitude (storm generated) events, indicating that the latter are mainly responsible for the statistically-inferred propagation. A decrease in speed from 400-450 km day^{-1} near Salina Cruz to 250-300 km day^{-1} near Manzanillo is consistent with southern forcing by storms, which typically travel with speeds of 340-520 km day^{-1}. North of Manzanillo, speeds remain near 270-310 km day^{-1} as far north as Mazatlan, then decrease to 190-250 km day^{-1} near Guaymas. The lower and more uniform speeds north of Manzanillo appear to be consistent with free coastal trapped waves supported by both stratification and topography. Free wave speeds, however, are functions of latitude, local shelf topography, stratification and perhaps amplitude, and the answer to (5) is still under study.

References

Allen, J. S. and R. D. Romea (1980) On coastal trapped waves in a stratified ocean. *Journal of Fluid Mechanics, 98,* 555-585.

Brink, K. H. (1982) A comparison of long coastal trapped wave theory with observations off Peru. *Journal of Physical Oceanography, 12,* 897-913.

Christensen, N., Jr. and Rene de la Paz (1982) A study of sub-inertial waves off the west coast of Mexico. *Deep-Sea Research,* submitted.

Smith, R. L. (1978) Poleward propagating perturbations in currents and sea level along the Peru coast. *Journal of Geophysical Research, 83,* 6083-6092.

David B. Enfield
John S. Allen
School of Oceanography
Oregon State University
Corvallis, OR 97331

Instabilities on the Equatorial Beta Plane

The equatorial ocean and the tropical atmosphere are regions of strong latitudinal current and wind shear, which results in instabilities at low latitudes. Kuo (1978) and Philander (1978) have studied the barotropic and baroclinic instability of zonal equatorial currents, while Dunkerton (1981) has discussed the inertial instability on the equatorial beta plane when the zonal wave number is zero.

This brief note will show that the equatorial Kelvin wave and gravity waves in horizontal shear are unstable. Rossby waves can also be unstable, but will not be studied here. The mean zonal flow U contains a linear shear in the north-south direction, *i.e.*, $U(y) = Sy$, where S is constant and y is the latitude. A linear shear is always barotropically stable according to the "Rayleigh-Kuo" criterion, thus "filtering out" unstable Rossby waves from our calculations. This linear shear makes it possible to separate variables and formulate our model, which consists of the linearized shallow water wave equations for an inviscid, stratified fluid on the equatorial beta plane. In nondimensional form, the model equations are (Boyd, 1980):

$$\begin{aligned} ivu - (y - \Gamma(y))v + ik\phi &= 0 \\ yu + ivv + \phi_y &= 0 \\ iku + v_y + ikv\phi &= 0 \end{aligned} \qquad (1)$$

where k is the zonal wavenumber; ν is the Doppler shifted frequency $(U(y) - c)\,k$; c is the phase speed of the waves; subscript y denotes differentiation with respect to latitude y; u and v are the zonal and meridional velocities, respectively; ϕ is the height; and $\Gamma(y) = dU/dy = S$.

This model is too simplified to allow a direct comparison with the viscous and diabatic atmosphere or ocean, where the dynamical and physical processes are very complicated. However, in terms of mathematical analysis, the model is sufficient to provide a basic understanding of the mechanisms that trigger instabilities in the equatorial region.

In an effort to reduce the calculations that arise in computing the complex eigenvalues, c, of equation (1), different approximations were introduced to gain some insight into the different modes of instability. Note that a phase speed with a positive imaginary part, c_{im}, characterizes an unstable wave that grows as $\exp(kc_{im}t)$, where t is time.

The first approximation is the "long wave approximation" (Boyd and Christidis, 1982), which filters out all gravity waves and eliminates the wavenumber k as an explicit parameter in our calculations. A shooting method was used for the computation of the